

Assessment of Negative Gingival Recession

Subjects: Dentistry, Oral Surgery & Medicine

Contributor: I-Ching Wang, Hsun-Liang Chan, Georgia K. Johnson, Satheesh Elangovan

Accurate measurement of negative gingival recession (GR) is essential to accurately determine the clinical attachment loss, which leads to an accurate diagnosis and optimal therapy of periodontal disease.

Keywords: negative gingival recession ; clinical attachment loss ; Ultrasonography

1. Introduction

The term, negative gingival recession (GR), indicates that the free gingival margin is coronal to the cemento-enamel junction (CEJ). It is an important component of the periodontal examination that allows the clinician to calculate the clinical attachment loss (CAL) to define disease severity and monitor disease progression. CAL represents the extent of periodontal tissue loss, which is measured as the distance from the CEJ to the base of the pocket ^[1] and is clinically calculated by deducting the distance of the gingival margin coronal to the CEJ from the pocket depth ^[2]. However, it involves some “guess work” to determine the amount of negative GR in relation to the CEJ position, and limited reproducibility and measurement errors have been reported in the literature ^{[3][4][5]}. Therefore, the early diagnosis of initial periodontitis can be challenging to clinicians, and the assignment of periodontitis severity and progressive changes of attachment level over time could be inconsistent.

2. Normal Anatomy

Preservation of an intact dentogingival unit with the gingival margin slightly coronal to the CEJ in a state of optimal health is a hallmark feature for an intact, healthy dentition. The biological interface between the gingiva and the tooth that forms the initial barrier to underlying tissues is known as the “dentogingival junction”(DGJ) ^[6]. The average dimension of sulcus depth, epithelial attachment, and the connective tissue attachment was reported to be 0.69 mm, 0.97 mm, and 1.07 mm, respectively ^[7]. Today, the latter two a functional unit, is termed the “supracrestal tissue attachment” ^[8] which was previously known as the “biologic width”.

The apical migration of the DGJ after dentition completes the active phase of eruption is called passive eruption ^[9]. Gargiulo et al. described the changes that occur in the location of DGJ in relation to the CEJ in four stages of passive eruption ^[7]. In stage I of the passive eruption, which represents a physiologically healthy state, the location of epithelial attachment (today called junctional epithelium) is entirely on the enamel with the most apical termination at the CEJ. The average gingival dimension coronal to the CEJ (negative GR) at stage I that comprises of sulcus depth and epithelial attachment is 2.15 mm ^[7]. Along with the apical shift of the dentogingival junction, which is considered a consequence of pathological periodontal destruction, the epithelial attachment is on the enamel and cementum at stage II and entirely located on the cementum at stage III until the epithelial attachment and gingival margin lie apical to the CEJ at stage IV ^{[7][10][11]}. The average gingival dimension coronal to the CEJ (negative GR) is 1.29 mm (sulcus and part of epithelial attachment) and 0.6 mm (purely sulcus depth) at stages II and III, respectively. In stage IV and beyond, the gingival margin is at the level of or apical to the CEJ. To sum up, the dimension described by Gargiulo et al. (stage I–III of passive eruption) is in accordance with the common understanding that the facial gingiva margin is approximately 0.5 to 2 mm coronal to the CEJ. This was based on the observation of the distance from free gingiva margin to the free gingival groove and the latter corresponds to the bottom of the gingiva crevice (the base of the epithelial attachment) that is often located at CEJ ^[12].

Normally, the scalloped osseous crest parallels the CEJ circumferentially. The osseous scallop (defined by the distance from the crestal bone level at the mid-buccal/lingual site to the crestal bone level at the interproximal site) is greatest at the maxillary anterior teeth, averaging 3.5 mm, and gradually flattens out posteriorly ^[13]. The extent of the osseous scallop is strongly associated with the bone morphotype and can range from 2.1 mm in a flat type to as high as 4.1 mm in a pronounced scalloped type ^[14]. On average, the distance from the gingival margin to the bone crest is about 3 mm at the mid-facial sites and ranges from 3 to 4.5 mm at interproximal sites in periodontally healthy patients depending on the

amount of gingival scallop in relation to the underlying interproximal osseous scallop [15]. Considering that the average distance from CEJ to the alveolar crest is 1.5 mm (range: 1.08 to 1.71 mm) in stages I to III of passive eruption [2], the interproximal papilla height coronal to the interproximal CEJ is between 2–3.5 mm on average, and is greater in patients with a thick phenotype.

3. Clinical Assessment Approaches

3.1. Manual Instrumentation

CAL is determined by taking into account the probing depth and GR measurements. In the site where a negative GR exists, the distance from the gingival margin to the CEJ is subtracted from the probing depth to determine the CAL. Whereas at sites with positive GR (gingival margin located apical to the CEJ), CAL is determined by adding the PD with the positive GR value [2]. Locating the CEJ in the presence of negative GR can be particularly challenging, and there is a degree of guesswork involved in this indirect clinical approach that is subject to measurement errors and variations between examiners. CEJ location in such an approach is determined based on crown anatomy (crown length and ratio of length/width), curvature of the CEJ, and visibility of the adjacent CEJ. In the literature, measurement errors in the range of 30–50% and 20–40% have been reported for CAL and pocket depth measures using the indirect approach, respectively [16][17][18][19].

Alternatively, the clinician can directly “reflect” the papilla by the periodontal probe to visualize or “feel” for the CEJ to assess the amount of negative recession. However, in some scenarios, the CEJ may not be visible or may lack a clear demarcation, leading to visual or tactile errors [20]. On the proximal surfaces, the partial vertical course of the CEJ further increases the difficulty in locating the CEJ [21]. In addition, it is usually not feasible in daily clinical practice to complete a periodontal chart by direct approach due to its time-consuming nature. Vision-enhancement methods, e.g., the use of the operating microscope, equipped with high magnification (10–25×) and co-axial illumination, could assist in identifying the CEJ for better negative-recession determination, but the availability of this tool for clinical use is currently limited (**Figure 1**). From a measurement-error point of view, direct measurements are less error-prone than the indirect approach. However, the intra- and inter-examiner variabilities are still very high and both these approaches can be time-consuming [22].



Figure 1. Visualization of negative recession using an operating microscope with magnification (10×) and co-axial illumination during ultrasonic scaling.

3.2. Automated Instrumentation

Several automatic electronic probes have been developed to address the high variability of PD and CAL. Jeffcoat et al. proposed a periodontal probe with automated CEJ detection function with controlled insertion force of 35 g [23]. Despite the high repeatability, it has been only used for research purposes [24]. Preshaw et al. modified an automated Florida probe and created a flange to detect CEJ [25], and it was proven to have increased inter-examiner consistency in detecting CAL [26][27]. However, later evidence indicated that electronic probes do not offer a substantially advantage to reduce measurement errors [28][29][30]. Although the electronic probe can overcome errors and some of the limitations of manual probes [31], the manual probe is easier to use, less time-consuming, economical, and can be walked circumferentially to identify the deepest pocket. These factors have limited the widespread use of electronic probes [32][33].

3.3. Imaging Technologies

Radiographic techniques including intra-oral radiography and cone-beam computed tomography (CBCT) have been employed to assess the soft-tissue dimension in relation to the CEJ, but the scatter radiation and low-contrast resolution of soft tissue and CEJ outline limits their use in determining negative GR [34][35]. Alternatively, dental ultrasonography, a noninvasive and nonionizing modality, has been proposed to image periodontal tissues [36]. Ultrasonography functions by transmitting sound waves from the ultrasound transducer (probe) through a medium and then recording time-dependent reflections from tissues to determine its dimensions. Efforts have been made to develop an ultrasonic device to measure periodontal pocket depths, but the approach has failed to demonstrate reproducibility [37]. The device consisted of a thin probe inserted into the sulcus that directs the sound wave into the pockets in the presence of water (for coupling), and a computer algorithm then identifies the junction between the junctional epithelium and the connective tissue via the impedance difference of returning echo signals which infers the depth of the periodontal pocket. More promising outcomes in mapping the periodontal tissue dimensions have come with the evolution of transducers with higher frequency (higher image resolution). These have included studies in porcine models [38][39][40][41], human cadavers [42][43], and live humans [44][45][46][47].

Recently, dental ultrasonography has been modernized to a miniature-sized (comparable to a toothbrush) ultrasound transducer suitable for use in the oral cavity with higher-frequency (24 MHz) and high-resolution imaging (**Figure 2**). Its accuracy in the evaluation of periodontal and peri-implant tissue dimensions was validated by comparing these measures to direct bone sounding and CBCT [47][48][49]. **Figure 3** provides an example of a cross-sectional scan at mid-facial and interproximal planes of a periodontal healthy maxillary central incisor using a modern commercially available ultrasound scanner (ZS3, Zonare, Mindray, Mahwah, NJ, USA) coupled with a 24 MHz miniature-sized imaging probe. In this example, the CEJ is clearly visualized and negative GR was measured to be 0.5 mm higher at distal papilla than at the mid-facial site. In contrast to probing, ultrasonography allows for noninvasive imaging of the CEJ and alveolar bone crest without the measurement variability caused by the inflamed gingiva tissues. Researchers know from earlier studies that inflammation greatly impacts the probing depth measurement with the probe going past the junctional epithelium in inflamed sites while stopping coronal to apical termination of junctional epithelium in noninflamed sites [50][51][52]. Most of the time, clinical attachment levels by probing are within 1 mm of the true histological level of the connective tissue attachment [53]. Although current B-mode ultrasound imaging cannot directly determine the true CAL, it can aid in its calculation by accurately measuring the amount of negative GR. This can supplement the clinical probing depth to calculate CAL directly. Alternatively the distance from the CEJ-bone crest can be measured by ultrasound, then the CAL can be indirectly calculated by subtracting 1 mm of average dimension of connective tissue attachment [7] from the CEJ-bone crest distance.

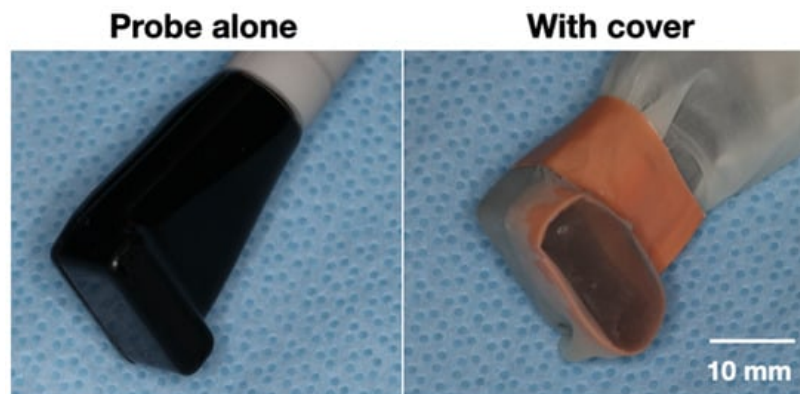


Figure 2. Modern miniature-sized ultrasound probe (transducer) with high frequency (24 MHz).

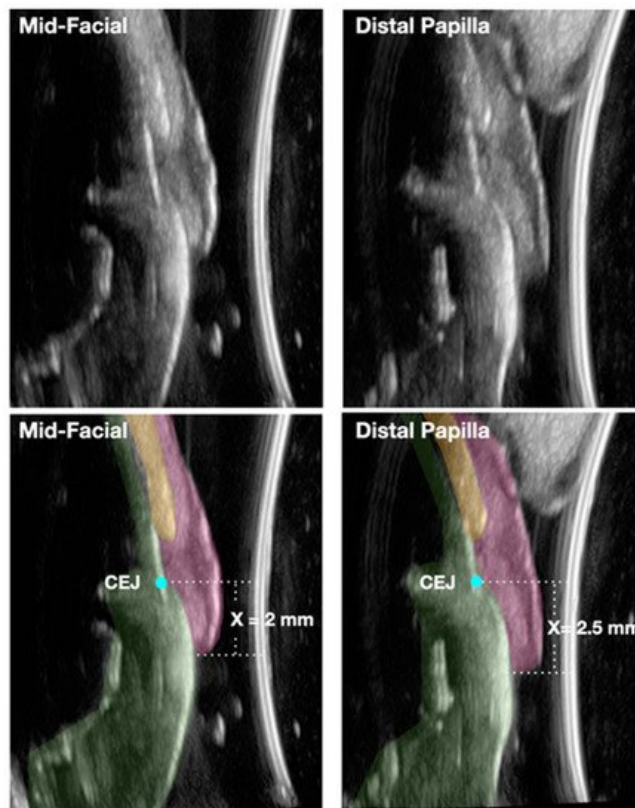


Figure 3. Example of an ultrasonographic cross-sectional image showing negative gingival recession on a maxillary central incisor. Colored areas represent different anatomic locations. Red: gingiva; yellow: alveolar bone; green: tooth. Cyan round point represents the CEJ. X measurements indicate the amount of negative gingiva recession.

4. Conclusion

- Measuring the amount of gingiva recession, both negative and positive, is an integral part of determining the clinical attachment loss.
- Detecting the CEJ has proven to be a challenge clinically when the gingival margin is coronal to the CEJ. To properly diagnose the amount of negative gingival recession, understanding the normal site-specific anatomy is the first step.
- With the aid of novel noninvasive and chairside ultrasound imaging and the high-magnification operating microscope, accurate and reproducible assessment of the negative gingival recession can become a reality that allows for early detection and intervention of periodontitis. These technologies could also prove to be valuable clinical and research tools in accurately detecting the amount of clinical attachment gain resulting from periodontal therapeutic modalities.

References

1. Listgarten, M.A. Re: Periodontal terminology. *J. Periodontol.* 1993, 64, 918.
2. Ramfjord, S.P. Indices for prevalence and incidence of periodontal disease. *J. Periodontol.* 1959, 30, 51–59.
3. Vandana, K.; Gupta, I. The location of cemento enamel junction for CAL measurement: A clinical crisis. *J. Indian Soc. Periodontol.* 2009, 13, 12–15.
4. Badersten, A.; Nilvéaus, R.; Egelberg, J. Reproducibility of probing attachment level measurements. *J. Clin. Periodontol.* 1984, 11, 475–485.
5. Hug, H.U.; Van't Hof, M.A.; Spanauf, A.J.; Renggli, H.H. Validity of clinical assessments related to the cemento-enamel junction. *J. Dent. Res.* 1983, 62, 825–829.
6. Sicher, H. Changing concepts of the supporting dental structures. *Oral Surg. Oral Med. Oral Pathol.* 1959, 12, 31–35.
7. Gargiulo, A.W.; Wentz, F.M.; Orban, B. Dimensions and relations of the dentogingival junction in humans. *J. Periodontol.* 1961, 32, 261–267.

8. Jepsen, S.; Caton, J.G.; Albandar, J.M.; Bissada, N.F.; Boucharad, P.; Cortellini, P.; Demirel, K.; de Sanctis, M.; Ercoli, C.; Fan, J. Periodontal manifestations of systemic diseases and developmental and acquired conditions: Consensus report of workgroup 3 of the 2017 World Workshop on the Classification of Periodontal and Peri-Implant Diseases and Conditions. *J. Clin. Periodontol.* 2018, 45, S219–S229.
9. Gottlieb, B.; Orban, B. Active and passive continuous eruption of teeth. *J. Dent. Res.* 1933, 13, 214.
10. Mele, M.; Felice, P.; Sharma, P.; Mazzotti, C.; Bellone, P.; Zucchelli, G. Esthetic treatment of altered passive eruption. *Periodontology 2000* 2018, 77, 65–83.
11. Newman, M.G.; Takei, H.; Klokkevold, P.R.; Carranza, F.A. *Newman and Carranza's Clinical Periodontology*; Elsevier Health Sciences: Amsterdam, The Netherlands, 2018.
12. Ainamo, J.; Löe, H. Anatomical characteristics of gingiva. A clinical and microscopic study of the free and attached gingiva. *J. Periodontol.* 1966, 37, 5–13.
13. Ash, M.M.; Nelson, S.J. *Wheeler's Dental Anatomy, Physiology and Occlusion*, 8th ed.; Saunderson Elsevier: St. Louis, MO, USA, 2003; p. 259.
14. Becker, W.; Ochsenbein, C.; Tibbetts, L.; Becker, B.E. Alveolar bone anatomic profiles as measured from dry skulls: Clinical ramifications. *J. Clin. Periodontol.* 1997, 24, 727–731.
15. Kois, J.C. Altering gingival levels: The restorative connection part I: Biologic variables. *Int. J. Periodontics Restor. Dent.* 1994, 6, 3–7.
16. Goodson, J.M. Clinical measurements of periodontitis. *J. Clin. Periodontol.* 1986, 13, 446–460.
17. Hill, E.G.; Slate, E.H.; Wiegand, R.E.; Grossi, S.G.; Salinas, C.F. Study design for calibration of clinical examiners measuring periodontal parameters. *J. Periodontol.* 2006, 77, 1129–1141.
18. Glavind, L.; Löe, H. Errors in the clinical assessment of periodontal destruction. *J. Periodontol. Res.* 1967, 2, 180–184.
19. Kingman, A.; Löe, H.; Ånerud, Å.; Boysen, H. Errors in measuring parameters associated with periodontal health and disease. *J. Periodontol.* 1991, 62, 477–486.
20. Watts, T. Constant force probing with and without a stent in untreated periodontal disease: The clinical reproducibility problem and possible sources of error. *J. Clin. Periodontol.* 1987, 14, 407–411.
21. Barendregt, D.S.; van der Velden, U.; Timmerman, M.F.; Bulthuis, H.M.; van der Weijden, F. Detection of the cemento-enamel junction with three different probes: An "in vitro" model. *J. Clin. Periodontol.* 2009, 36, 212–218.
22. Corraini, P.; Baelum, V.; Lopez, R. Reliability of direct and indirect clinical attachment level measurements. *J. Clin. Periodontol.* 2013, 40, 896–905.
23. Jeffcoat, M.K.; Jeffcoat, R.L.; Jens, S.C.; Captain, K. A new periodontal probe with automated cemento-enamel junction detection. *J. Clin. Periodontol.* 1986, 13, 276–280.
24. Jeffcoat, M.K.; Jeffcoat, R.L.; Captain, K. A periodontal probe with automated cemento--enamel junction detection--design and clinical trials. *IEEE Trans. Biomed. Eng.* 1991, 38, 330–333.
25. Preshaw, P.M.; Kupp, L.; Hefti, A.F.; Mariotti, A. Measurement of clinical attachment levels using a constant-force periodontal probe modified to detect the cemento-enamel junction. *J. Clin. Periodontol.* 1999, 26, 434–440.
26. Karpinia, K.; Magnusson, I.; Gibbs, C.; Yang, M.C. Accuracy of probing attachment levels using a CEJ probe versus traditional probes. *J. Clin. Periodontol.* 2004, 31, 173–176.
27. Deepa, R.; Prakash, S. Accuracy of probing attachment levels using a new computerized cemento-enamel junction probe. *J. Indian Soc. Periodontol.* 2012, 16, 74–79.
28. Wang, S.F.; Leknes, K.N.; Zimmerman, G.J.; Sigurdsson, T.J.; Wikesjö, U.M.; Selvig, K.A. Intra-and inter-examiner reproducibility in constant force probing. *J. Clin. Periodontol.* 1995, 22, 918–922.
29. Hefti, A.F. Periodontal Probing. *Crit. Rev. Oral Biol. Med.* 1997, 8, 336–356.
30. Trombelli, L.; Farina, R.; Silva, C.O.; Tatakis, D.N. Plaque-induced gingivitis: Case definition and diagnostic considerations. *J. Periodontol.* 2018, 89 (Suppl. 1), S46–S73.
31. Quirynen, M.; Callens, A.; van Steenberghe, D.; Nys, M. Clinical evaluation of a constant force electronic probe. *J. Periodontol.* 1993, 64, 35–39.
32. Perry, D.A.; Taggart, E.J.; Leung, A.; Newburn, E. Comparison of a conventional probe with electronic and manual pressure-regulated probes. *J. Periodontol.* 1994, 65, 908–913.
33. Bareja, H.; Bansal, M.; Naveen Kumar, P.G. Comparative assessment of conventional periodontal probes and CEJ handpiece of electronic probes in the diagnosis and primary care of periodontal disease. *J. Fam. Med. Prim. Care*

34. Brezniak, N.; Goren, S.; Zoizner, R.; Shochat, T.; Dinbar, A.; Wasserstein, A.; Heller, M. The accuracy of the cemento-enamel junction identification on periapical films. *Angle Orthod.* 2004, 74, 496–500.
35. Patcas, R.; Markic, G.; Müller, L.; Ullrich, O.; Peltomäki, T.; Kellenberger, C.J.; Karlo, C.A. Accuracy of linear intraoral measurements using cone beam CT and multidetector CT: A tale of two CTs. *Dentomaxillofac. Radiol.* 2012, 41, 637–644.
36. Ghorayeb, S.R.; Bertoncini, C.A.; Hinders, M.K. Ultrasonography in dentistry. *IEEE Trans. Ultrason. Ferroelectr. Freq. Control* 2008, 55, 1256–1266.
37. Lynch, J.; Hinders, M. Ultrasonic device for measuring periodontal attachment levels. *Rev. Sci. Instrum.* 2002, 73, 2686–2693.
38. Tsiolis, F.I.; Needleman, I.G.; Griffiths, G.S. Periodontal ultrasonography. *J. Clin. Periodontol.* 2003, 30, 849–854.
39. Chifor, R.; HedeÅÿiu, M.; Bolfa, P.; Catoi, C.; Crisan, M.; Serbanescu, A.; Badea, A.F.; Moga, I. The evaluation of 20 MHz ultrasonography, computed tomography scans as compared to direct microscopy for periodontal system assessment. *Med. Ultrason.* 2011, 13, 120–126.
40. Nguyen, K.-C.T.; Le, L.H.; Kaipatur, N.R.; Zheng, R.; Lou, E.H.; Major, P.W. High-resolution ultrasonic imaging of dento-periodontal tissues using a multi-element phased array system. *Ann. Biomed. Eng.* 2016, 44, 2874–2886.
41. Chifor, R.; Badea, M.E.; Hedesiu, M.; Serbanescu, A.; Badea, A.F. Experimental model for measuring and characterisation of the dento-alveolar system using high frequencies ultrasound techniques. *Med. Ultrason.* 2010, 12, 127–132.
42. Mahmoud, A.M.; Ngan, P.; Crout, R.; Mukdadi, O.M. High-resolution 3D ultrasound jawbone surface imaging for diagnosis of periodontal bony defects: An in vitro study. *Ann. Biomed. Eng.* 2010, 38, 3409–3422.
43. Chan, H.-L.; Sinjab, K.; Chung, M.-P.; Chiang, Y.-C.; Wang, H.-L.; Giannobile, W.V.; Kripfgans, O.D. Non-invasive evaluation of facial crestal bone with ultrasonography. *PLoS ONE* 2017, 12, e0171237.
44. Zimbran, A.; Dudea, S.M.; Dudea, D. Evaluation of periodontal tissues using 40MHz ultrasonography. preliminary report. *Med. Ultrason.* 2013, 15, 6–9.
45. Salmon, B.; Le Denmat, D. Intraoral ultrasonography: Development of a specific high-frequency probe and clinical pilot study. *Clin. Oral Investig.* 2012, 16, 643–649.
46. Nguyen, K.-C.T.; Yan, Y.; Kaipatur, N.R.; Major, P.W.; Lou, E.H.; Punithakumar, K.; Le, L.H. Computer-Assisted Detection of Cemento-Enamel Junction in Intraoral Ultrasonographs. *Appl. Sci.* 2021, 11, 5850.
47. Tattan, M.; Sinjab, K.; Lee, E.; Arnett, M.; Oh, T.J.; Wang, H.L.; Chan, H.L.; Kripfgans, O.D. Ultrasonography for chairside evaluation of periodontal structures: A pilot study. *J. Periodontol.* 2020, 91, 890–899.
48. Siqueira, R.; Sinjab, K.; Pan, Y.C.; Soki, F.; Chan, H.L.; Kripfgans, O. Comprehensive peri-implant tissue evaluation with ultrasonography and cone-beam computed tomography: A pilot study. *Clin. Oral Implant. Res.* 2021, 32, 777–785.
49. Chan, H.L.; Sinjab, K.; Li, J.; Chen, Z.; Wang, H.L.; Kripfgans, O.D. Ultrasonography for noninvasive and real-time evaluation of peri-implant tissue dimensions. *J. Clin. Periodontol.* 2018, 45, 986–995.
50. Magnusson, I.; Listgarten, M.A. Histological evaluation of probing depth following periodontal treatment. *J. Clin. Periodontol.* 1980, 7, 26–31.
51. Fowler, C.; Garrett, S.; Crigger, M.; Egelberg, J. Histologic probe position in treated and untreated human periodontal tissues. *J. Clin. Periodontol.* 1982, 9, 373–385.
52. Armitage, G.C.; Svanberg, G.K.; Löe, H. Microscopic evaluation of clinical measurements of connective tissue attachment levels. *J. Clin. Periodontol.* 1977, 4, 173–190.
53. Armitage, G.C. Manual periodontal probing in supportive periodontal treatment. *Periodontology* 2000 1996, 12, 33–39.